

GCOM-C1/SGLI Land Surface Temperature Product
Algorithm Theoretical Basis Document

Masao Moriyama
Nagasaki University
Nagasaki, JAPAN.

May 28, 2020

Contents

1	Introduction	1
2	LST estimation algorithm	2
2.1	Physics of the LST estimation algorithm	2
2.2	SGLI LST Split window algorithm	2
2.3	Semi-analytical LST estimation algorithm	4
2.3.1	Overview	4
2.3.2	Integration of the split window method and semi-analytical method	4
2.3.3	Numerical validation	5
3	Operation	6
3.1	Input/Output Dataset	6
3.2	QA plane	6
4	Validation	8
4.1	Overview	8
4.2	LST from longwave radiation measurement at the flux site	8

List of Figures

2.1	SGLI TIR channels	3
2.2	3 types of the split window coefficient sets	3
2.3	Regression error of the SGLI IST split window formula (Left: Comparison between model and estimated LST, Right: error histogram)	4
2.4	Comparison of the model and estimated LST (Left) and the LST estimation error summary (Right)	5
4.1	Schematic of the flux site	8
4.2	Flux site used for SGLI LST validation	9
4.3	Comparison between the SGLI LST and the longwave radiation based LST	10
4.4	SGLI LSTQA (Left), LST(Center) and RGB(Right) around Albuquerque, NM on June 18, 2018	10

List of Tables

2.1	Numerical simulation for the split window coefficients definition	3
2.2	The semi-analytical method simulation condition	5
3.1	The input dataset	6
3.2	The output dataset	6
3.3	SGLI LST QA plane	7
4.1	Fluxsites for the SGLI LST validation	9

Chapter 1

Introduction

This document describes the land surface temperature estimation algorithm for SGLI sensor. So far the land surface temperature estimation from space is made by many kinds of sensors, as the operational product, ASTER and MODIS onboard TERRA satellite made the land surface temperature product in late 90's. Just after this, ATSR onboard the European satellite ESA published the land surface product. The operational land surface temperature estimation has about 20 years history and the improvement of the estimation algorithm are made.

For SGLI, the land surface temperature estimation algorithm will be made on the basis of these previous algorithm and will be added the new improvement. The split window algorithm is used for MODIS and AATSR, this is less computation time and suitable for the wide swath sensor but the surface emissivity has to be the known variable. On the other hand, ASTER uses the semi-analytical method to estimate not only the surface temperature but the emissivity, but it's computation time consumable. For SGLI, the semi-analytical method which uses the split window algorithm as the constraint of the land surface temperature/emissivity and the observed brightness temperature.

From the next chapter, the semi-analytical algorithm with the split-window formula will be described. And also the operational factor such as input and output and the data processing flow will be explained. At the end of this document, the validation plan will be noticed.

Chapter 2

LST estimation algorithm

2.1 Physics of the LST estimation algorithm

The satellite detected radiance at i th. observation channel I_i is described as the following radiative transfer equation.

$$I_i = \tau_i(\theta)I_{si} + I_{ai}(\theta) \quad (2.1)$$

where τ , θ , I_s and I_a are the total transmittance, the observation zenith, the land leaving radiance and the path radiance respectively. And the land leaving radiance is expressed as Eq. (2.2).

$$I_{si} = \varepsilon_i B_i(T_s) + (1 - \varepsilon_i) \frac{F_i}{\pi} \quad (2.2)$$

where ε , B , T_s and F are the surface emissivity, Planck function, the surface temperature and the downward atmospheric irradiance respectively. Even the atmospheric condition is known, the land leaving radiance contains two kinds of unknowns, surface temperature and emissivity. Since the surface emissivity has the spectral dependency, this problem is underdetermine in any numbers of the observation spectral channels.

The previous operational LST products have been made by 2 kinds of algorithm, the split window and the semi-analytical algorithm. The split window algorithm which is the multiple variable regression of the surface temperature, emissivity and the observed brightness temperature is used by the wide swath sensor such as MODIS, AATSR and VIIRS. The precondition of the split window algorithm is the surface emissivity have to be known. The semi-analytical algorithm which solve the simultaneous formulae of the land leaving radiance at each channel (Eq. (2.2)) and the additional equation is used by ASTER which has 5 spectral channels in TIR region. In the ASTER LST estimation algorithm case the additional equation is the emperical relationship between the statistical variables of the speectral emissivity. The precondition of the semi-analytical algorithm is the radiometric parameters such as the total transmittance, the path radiance and the downward atmospheric irradiance have to be known.

By comparing the preconditions of the two previous LST estimation algorithm, The radiometric parameter computation can be made by using the numerical foreacsting data, although the surface emissivity definition is difficult. So that the SGLI LST estimation algorithm uses the semi-analytical algorithm which add the split window formula to the land leaving radiance formulae at two SGLI TIR channels.

2.2 SGLI LST Split window algorithm

As the additional formula of the semi-analytical LST estimation algorithm, the split window formula have to contain the LST, emissivity and the observed brightness temperature at channels T1 and T2 (*cf.* Figure 2.1) explicitly.

To meet the condition of the additional formulae, the following function type of the sploit window formula is defined.

$$T_s = A_0 + (A_1 r_1 + A_2) T b_1 + A_3 r_1 + (A_4 r_2 + A_5) T b_2 + A_6 r_2 \quad (2.3)$$

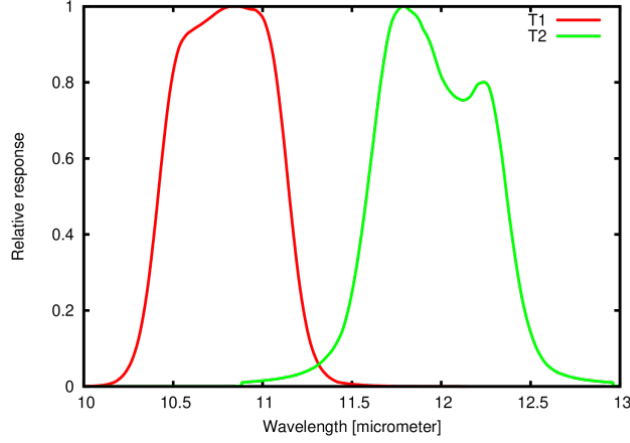


Figure 2.1: SGLI TIR channels

where Tb_1 and Tb_2 are the brightness temperature at channels T1 and T2, As are the regression coefficients and r are the surface reflectivity ($r_i = 1 - \varepsilon_i$, $i = 1, 2$).

To define the coefficients, the following numerical simulation (*cf.* Table 2.1) are made.

Table 2.1: Numerical simulation for the split window coefficients definition

Profile: ECMWF 2000 Monthly mean profile (averaged over 10 [deg.] latitude interval)
Surface temperature: Air temperature at the surface + 0, 5, 10, 15, 20, 25, 30[K]
Average emissivity $\bar{\varepsilon}$: 0.95, 0.96, 0.97, 0.98, 0.99, 1
Emissivity wavelength dependence a : -0.5, 0.25, 0, 0.25, 0.5
Observation zenith: 0, 15, 30, 45[deg.]

As the emissivity expression, the average emissivity $\bar{\varepsilon}$ and the emissivity wavelength dependence a as Eq. (2.4, 2.5) are used.

$$\bar{\varepsilon} = \frac{\varepsilon_1 + \varepsilon_2}{2} \quad (2.4)$$

$$a = \frac{\varepsilon_1 - \varepsilon_2}{2(1 - \bar{\varepsilon})}, \quad (\bar{\varepsilon} < 1) \quad (2.5)$$

To suppress the regression error of the split window formula, SGLI LST estimation algorithm uses the 3 types of the split window coefficient set as shown in Figure 2.2.

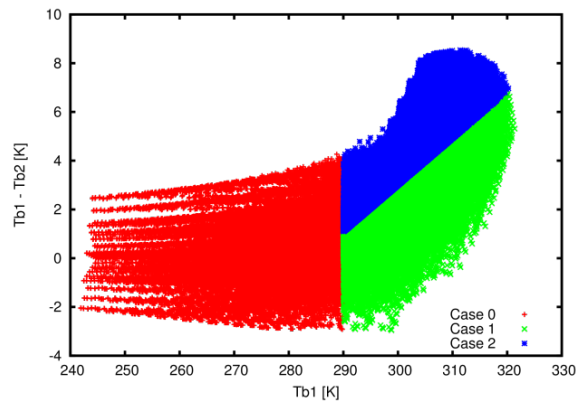


Figure 2.2: 3 types of the split window coefficient sets

The regression error of the split window formulae are shown in Figure 2.3, Even in the worst case, the regression error is about 1.5[K] and it is sufficient for the semi-analytical LST estimation algorithm.

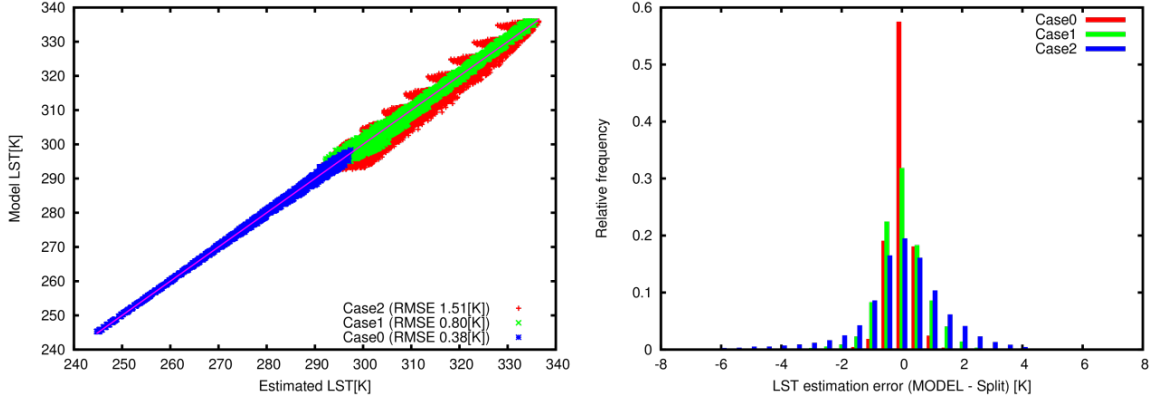


Figure 2.3: Regression error of the SGLI LST split window formula (Left: Comparison between model and estimated LST, Right: error histogram)

2.3 Semi-analytical LST estimation algorithm

2.3.1 Overview

As explained before, the land leaving radiance (*cf.* Eq. (2.2)) has two unknowns, the surface temperature and emissivity, and the surface emissivity has spectral dependency. Since this problem becomes underdetermined, reduction of the unknown or addition of the extra formula is necessary to solve this problem. ASTER LST estimation algorithm uses the additional formula which is defined from the statistics of the spectral emissivity of the 5 TIR observation channels. But for the less observation channel sensor such as AVHRR, MODIS, there were no additional formula because the two observation channels are not enough to establish the spectral emissivity relationship.

2.3.2 Integration of the split window method and semi-analytical method

From the other viewpoint, the SGLI LST split window formula is regarded as the statistical relationship between the observed value and the unknown variables and it has the enough accuracy so that this formula can be the additional formula to the semi-analytical method. In this case, since the split window method contains the satellite detected brightness temperature, the following simultaneous equation (Eq. (2.6 – 2.8)) which contains the radiative transfer equation which expresses the satellite detected brightness temperature instead of the land leaving radiance.

$$Tb_1 = B_1^{-1}[\tau_1(\varepsilon_1 B_1(T_s) + (1 - \varepsilon_1)\frac{F_1}{\pi}) + I_{a1}] \quad (2.6)$$

$$Tb_2 = B_2^{-1}[\tau_2(\varepsilon_2 B_2(T_s) + (1 - \varepsilon_2)\frac{F_2}{\pi}) + I_{a2}] \quad (2.7)$$

$$T_s = (A_1 + A_2 r_1)Tb_1 + A_3 r_1 + (A_4 + A_5 r_2)Tb_2 + A_6 r_2 + A_0 \quad (r_i = 1 - \varepsilon_i) \quad (2.8)$$

where B^{-1} is the Inverse Planck function. Among this simultaneous equation, the brightness temperature Tb_1 and Tb_2 are the observed value, the transmittance τ , the path radiance I_a and the downward atmospheric irradiance F is the computed value from the atmospheric condition and the surface temperature T_s and the emissivity ε are the solutions. To solve this simultaneous equation, the Newtonian iteration scheme is used.

2.3.3 Numerical validation

For the accuracy verification, the LST estimation using the numerical simulated observed radiance is made. The simulation condition is listed in Table 2.2. The terminate condition of the iteration scheme is the RMS residual of the cost function, Eqs. (2.6 – 2.8) or the number of the iteration. If the RMS residual is less then 0.5[K] of the number of the iteration reaches to 10, the computation is terminated.

Table 2.2: The semi-analytical method simulation condition

Atmospheric profile	Longitudinal mean with 10° latitude interval of 2000 ECMWF monthly mean atmosphere
$\bar{\epsilon}$	0.94, 0.95, 0.96, 0.97, 0.98, 0.99
a	-0.5, -0.25, 0, 0.25, 0.5
Surface temperature	Surface air temperature + 0, 5, 10, 15 [K]
Observation zenith	0, 15, 30, 45°
Observation error	0.2 [K] (@300 [K]): twice of the nominal value
Max. iteration number	10

The comparison between the model and estimated LST and the error summary under the various RMS residual and the trasmittance of channel T1 are shown in Figure 2.4.

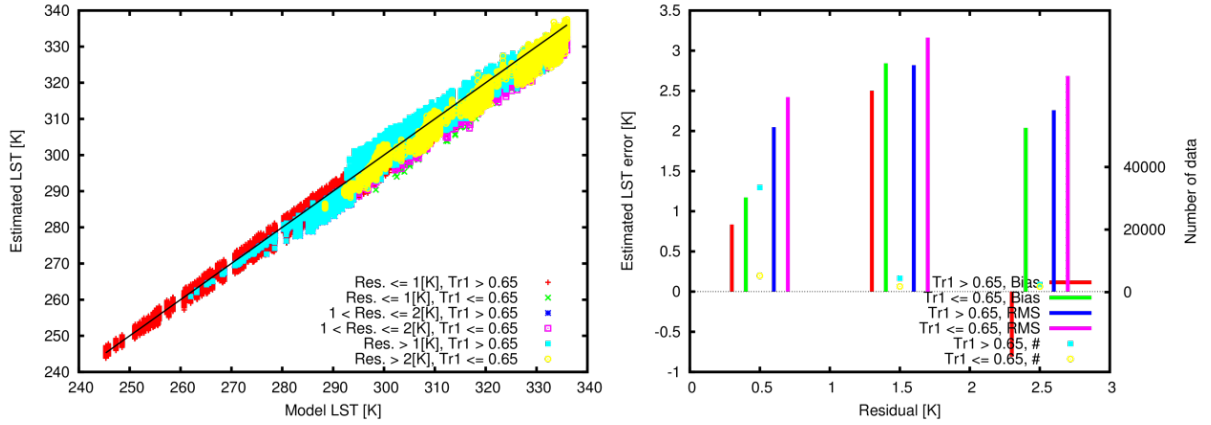


Figure 2.4: Comparison of the model and estimated LST (Left) and the LST estimation error summary (Right)

From the results, the proposed LST estimation algorithm has the enough accuracy and the RMS residual of the const function and the trasmittance indicate the estimation accuracy.

Chapter 3

Operation

3.1 Input/Output Dataset

The input dataset for LST estimation algorithm are summarized in Table 3.1.

Table 3.1: The input dataset

	Dataset
a	Precise geometrically corrected radiance (SGLI LTOAQ: 250[m] resolution)
b	Pixel wise Latitude and Longitude (To access the numerical forecasting data)
c	Pixel wise scan zenith angle (in LTOAQ: 250 [m])
d	Cloud flag (SGLI CLFGQ: 250[m] resolution)
e	Land mask (in LTOAQ: 250[m])
f	Elevation
g	Nearest time numerical forecasting data (pressure, height, temperature, humidity) (Japan Meteorological Agency Grid Point Value: 6 hours interval, 0.5 [deg.] resolution)

The output dataset are summarized in Table 3.2. These are stored in product HDF file as an independent plane.

Table 3.2: The output dataset

	Dataset
A	Land surface temperature
B	Land surface emissivity at 10.8 [μm]
C	Land surface emissivity at 12.0 [μm]
D	QA

3.2 QA plane

The QA plane of SGLI/LST product is 2 bytes per pixel. The lower byte contains the information for the level 3 data production and the upper byte contains the LST quality related information. The QA plane are described in Table 3.3.

The upper byte of the QA plane is designed as the “Smaller the better concept”, this means the smaller value of the upper byte shows the more accurate LST product.

Table 3.3: SGLI LST QA plane

Bit	Contents	Bit	contents
00	No input data	08	T1 transmittance is less than 0.6
01	Land/Water (0: land, 1: water)	09	The residual is within the range of 1 to 2 [K]
02	Spare	10	The residual is larger than 2 [K]
03	Spare	11	Probably cloudy
04	no VNIR	12	Cloudy
05	Snow	13	LST is out of range
06	Sensor zenith is larger than 33[deg.]	14	Land/Water (0: land, 1: water)
07	Sensor zenith is larger than 43[deg.]	15	No input data

Chapter 4

Validation

4.1 Overview

By comparing with the ocean buoy data which is used for the sea surface temperature product validation, there are very few ground measured LST dataset. For SGLI LST product validation, the upward and downward longwave irradiance data measured at the flux site are mainly used, in addition the ground measured LST data at the same time of the satellite passing are used.

4.2 LST from longwave radiation measurement at the flux site

For the constant monitoring of the energy and the material flux near the surface, the various instruments are installed in one place, such place is called the flux site. The schematic of the flux site is shown in Figure 4.2. Among the instruments, some sites install the 4 component radiometer which measure the upward and downward short and longwave irradiance.

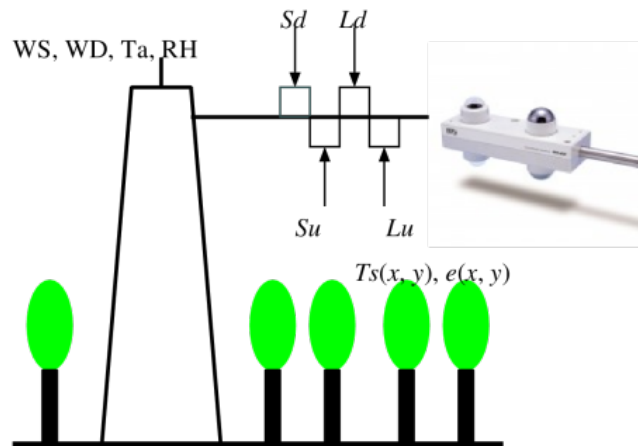


Figure 4.1: Schematic of the flux site

The relationship of the upward and downward longwave irradiance Lu , Ld the broadband emissivity e and LST are formulated as Eq. (4.1)

$$Lu = e\sigma Ts^4 + (1 - e)Ld \quad (4.1)$$

where σ is Stefan–Boltzmann constant. From the longwave radiation data, LST is computed at the satellite passing time.

During 2018 to 2019, the flux site in US and Canada listed in Table 4.1 are used for the SGLI LST product validation (*cf.* Figure 4.2). In this case the broadband emissivity is defined as constant 0.98.

Table 4.1: Fluxsites for the SGLI LST validation

Name	Tile	Cover	Name	Tile	Cover
US-Rls	V04H09	CSH	US-Me6	V04H09	ENF
US-NR1	V04H09	ENF	US-Rws	V04H09	OSH
CA-DBB	V04H09	WET	US-Ne1	V04H10	CRO
US-Ne2	V04H10	CRO	US-Ne3	V04H10	CRO
US-Ro5	V04H11	CRO	US-Ro6	V04H11	CRO
US-WCr	V04H11	DBF	US-Ro4	V04H11	GRA
US-Syv	V04H11	MF	US-Los	V04H11	WET
US-UMB	V04H12	DBF	US-UMd	V04H12	DBF
US-xBR	V04H12	DBF	US-xHA	V04H12	DBF
US-PHM	V04H12	WET	US-Ho1	V04H13	ENF
US-Tw3	V05H08	CRO	US-Tw1	V05H08	WET
US-Tw4	V05H08	WET	US-Mpj	V05H09	ENF
US-Vcp	V05H09	ENF	US-Seg	V05H09	GRA
US-Ses	V05H09	OSH	US-Wjs	V05H09	SAV
US-ARM	V05H10	CRO	US-xKZ	V05H10	GRA
US-MMS	V05H11	DBF	US-NC2	V05H11	ENF
US-NC3	V05H11	ENF	US-NC4	V05H11	WET
US-KS3	V06H10	WET			

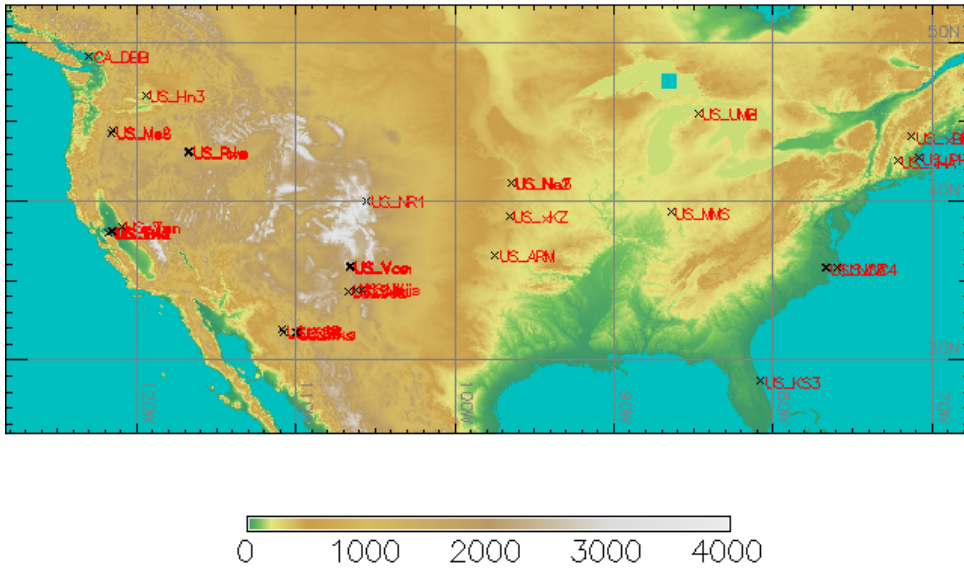


Figure 4.2: Flux site used for SGLI LST validation

From the flux site data, 1303 truth data are available, and from the comparison between SGLI and truth LST, it is clarify that the bias error is 0.47[K] and RMS error 2.36[K] (*cf.* Figure 4.3). It satisfies the success criteria. As the processing example, SGLI LST, QA and RGB composite around Albuquerque, NM on June 18, 2018 are shown in Figure 4.4.

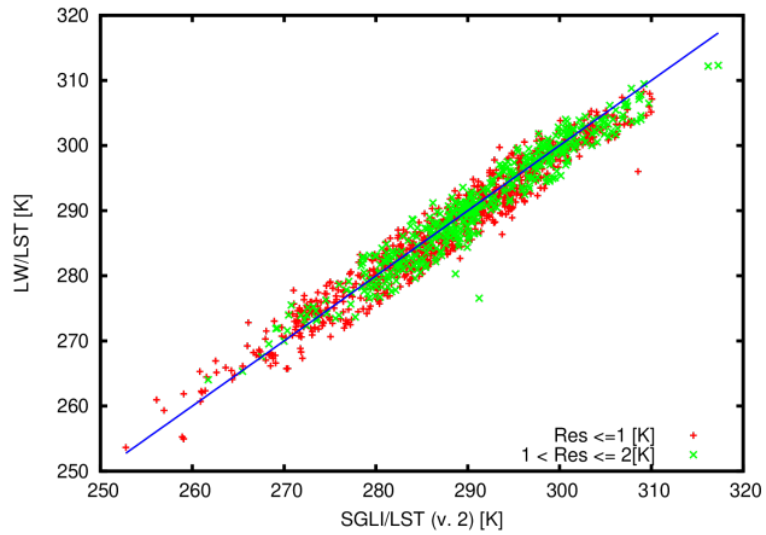


Figure 4.3: Comparison between the SGLI LST and the longwave radiation based LST

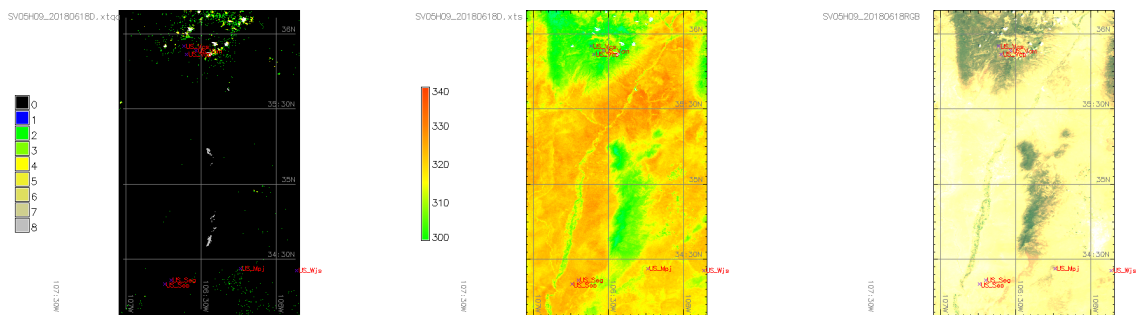


Figure 4.4: SGLI LSTQA (Left), LST(Center) and RGB(Right) around Albuquerque, NM on June 18, 2018